

A TIME DISCONTINUOUS PROCEDURE FOR THE HYDRAULIC CRACK SIMULATION IN COHESIVE POROUS MEDIA

Stefano Secchi^{1,2}, Luciano Simoni², Bernard Schrefler²

¹ CNR - ISIB,

Corso Stati Uniti 4, 35127 Padova, Italy

² Department of Structural and Transportation Engineering, University of Padua
Via Marzolo 9, 35121 Padova, Italy

secchi@isib.cnr.it

Abstract

Traditional phenomenological constitutive relationships sometimes fail in the description of mechanical behavior of plain concrete. In such circumstances more refined models are necessary, which takes into account the multiphase structure of the material. This paper presents a generalized finite element formulation, which incorporates solid and fluid phases together with a temperature field. The model is developed to obtain time-dependent solutions of 2-D cases, such as concrete gravity dams subjected to loading-unloading cycles, non-homogeneous specimens subjected to thermo-mechanical effects, etc. A fully coupled cohesive-fracture discrete model, which includes thermal and hydraulic loads, is adopted to describe crack nucleation and propagation. The evolution of fractures leads to continuous topological changes of the domain and these are handled by systematic local remeshing of the domain and by a continuous change of fluid and thermal boundary conditions. In the adopted approach, cracks may nucleate everywhere depending only on the stress field and propagate along paths and with a velocity of the tip that is a priori unknown. An adaptive remeshing technique for the spatial domain coupled with an adaptive procedure in time, based on the use of time-discontinuous finite elements, is used. The solution procedure is discussed in particular as far as the projection of the solution between two successive meshes is concerned.

Keywords: Hydraulic fracture, Discontinuous Galerkin, Adaptive Remeshing.

Presenting Author's biography

Stefano Secchi obtained a Structural Engineering degree at the Engineering Faculty of the University of Padova, Italy, in 1993, with a thesis on computational methods for the numerical simulation cohesive materials. He had a PhD degree in Structures Mechanics in 1997, discussing a thesis on computational methods for crack simulation in porous materials. From 1998 he works in the field of computational mechanics of porous media. He is currently researcher at ISIB CNR, Padova, Italy.



1 Introduction

In the study of coupled phenomena with interactions between mechanical, fluid and thermal fields in quasi-static or dynamic conditions it is very difficult to optimize *a priori* geometrical mesh and time stepping. The first one is a consequence of model singularities (i.e. boundary conditions, fracture propagation, material non linearities and geometrical singularities). The second one is determined by numerical properties of solution (stability and accuracy). A great number of consolidated methods for automatic space refinement based on *a posteriori* error measurements [1] is available in the literature instead, about time stepping, an effective method is still to be found, in particular in presence of interactive fields that can influence the time stepping itself.

An automatic adaptive procedure in the space and time domain for the analysis of mechanical behaviour of multi-phase systems is presented. The study is referred to cohesive fracture propagation, hydraulic and thermal, in 2-D domains of any shape, homogeneous or not.

The fracture propagation is simulated continuously updating the geometry and refining automatically the mesh with techniques that take into account appropriate error indicators. The analysis is developed through subdomains, in some of them the nucleation and propagation of cohesive fracture develop, in the others a linear elastic constitutive model for the material is assumed [2].

The adaptive procedure in space uses an automatic remeshing algorithm based on a Delaunay triangulation with a topological structure particularly effective for the analysed problems [3].

The adaptive procedure in time has resort to time-discontinuous finite elements, with *Galerkin* approximation techniques.

The approximations in each time step are based on linear functions; the unknown values are the field variables at the beginning and at the end of the time step. The continuity of the solution in time domain is imposed in a weak form, according to the standard finite element method statement.

The proposed method is particularly flexible and very effective when a continuous change of geometrical mesh and time stepping is requested. Among the advantages of the proposed method when compared to traditional integration methods based on finite differences (with the same order of approximation) the most remarkable are the improved accuracy, the mitigation of the spurious oscillations of the solution typical in traditional time integration algorithms with incompressible fluids, the reduction of oscillations due to high modes. However, the most interesting aspect is the possibility to define an error measure based on the discontinuity of the solu-

tion at the beginning of time steps in order to activate a time stepping procedure. The drawbacks of the proposed procedure are essentially computational, in fact the number of unknowns is doubled and the final system of discretized equation turns to be non symmetric. Both these aspects can be certainly overtaken with the continuously increasing of the computational capabilities.

2 Governing equations

In what follows a basic constitutive model based on the hypothesis of linear elastic behaviour of the solid skeleton and the fully saturated media is presented [4]. The assumed model describes a solid porous material, fully saturated by the permeating fluid phase. Under this hypothesis the total stress σ_{ij} in the body is given by the sum of the hydrostatic pressure p and the effective stress σ'_{ij} applied to the solid skeleton:

$$\sigma'_{ij} = \sigma_{ij} + p\delta_{ij} \quad (1)$$

The constitutive model relating strain and effective stress acting on the solid phase is represented by the Hooke's law defining an isotropic, linear elastic material:

$$\begin{aligned} \sigma'_{ij} &= D_{ijkl} \left(\varepsilon_{kl} + \frac{p}{3K_s} \delta_{kl} \right) = \\ &= \left[\lambda \delta_{ij} \delta_{kl} + \mu (\delta_{ik} \delta_{il} + \delta_{il} \delta_{jk}) \right] \left(\varepsilon_{kl} + \frac{p}{3K_s} \delta_{kl} \right) \end{aligned} \quad (2)$$

where μ , λ are the Lamè's constants. The sum of diagonal strain tensor components represents the volumetric deformation of the solid grains and is related to the fluid pressure, being K_s the solid bulk modulus.

Because of the relevant frictional resistance given by the solid matrix, the motion of the fluid can be described in terms of a quasi-static approach. The three-dimensional flux is governed by the extension of the well-known Darcy's law:

$$v_i = K_{ii} (-p_{,i} + \rho_f g_i) \quad (3)$$

being v_i the components of the relative velocity of the fluid with respect to the solid phase and ρ_f the density of the fluid. The terms g_i indicate the components of the gravity acceleration while K_{ii} are the terms of the diagonal dynamic permeability matrix; $p_{,i}$ is the gradient of the hydrostatic pressure. The balance of momentum, in local form, is given by:

$$\sigma_{ij,j} - \rho \ddot{u}_i = f_i \quad \sigma'_{ij} = \sigma'_{ji} \quad (4)$$

where f_i represents the components of the body forces, u is the solid displacement and ρ is the density of the mixture. One assumes that the forces on the boundary Γ of the continuum body are defined on the subset Γ_σ , while displacements are fixed on the subset Γ_u , fulfilling the conditions: $\Gamma_\sigma \cup \Gamma_u = \Gamma$ and $\Gamma_\sigma \cap \Gamma_u = 0$. The balance of traction on Γ_σ completes the set of equations (4):

$$\sigma_{ij} n_j = t_i \quad (5)$$

where n_j define the outward normal in a generic point of Γ_σ and t_i are components of the imposed traction vector in the same point. The continuity equation of the fluid phase is given by:

$$\left(\rho_f v_i\right)_{,i} + \frac{\partial \rho_f}{\partial t} = 0 \quad (6)$$

The second term of the left-hand side take into account different contributions. When considering the density of fluid as constant in time and by taking into account the Darcy's law the previous balance equation can be expressed as:

$$\begin{aligned} & \left[K_{ii} (-p_{,i} + \rho_f g_i) \right]_{,i} + \left(\delta_{lk} - \frac{1}{3K_s} \delta_{ji} D_{ijkl} \right) \frac{\partial \varepsilon_{kl}}{\partial t} + \\ & + \left(\frac{1-n}{K_s} + \frac{n}{K_f} - \frac{1}{(3K_s)^2} \delta_{ji} D_{ijkl} \delta_{kl} \right) \frac{\partial p}{\partial t} + q = 0 \end{aligned} \quad (7)$$

where K_f is the bulk modulus of the fluid phase, q the flux term of the liquid phase and n is the porosity (ratio of fluid volume and total volume). The local form of the continuity equation must be coupled with the boundary conditions upon the pressure of the fluid phase and its flux:

$$\begin{aligned} p &= p_o \quad \text{on } \Gamma_p \\ v_i n_i &= K_{ii} (-p_{,i} + \rho_f g_i) n_i = q \quad \text{on } \Gamma_q \end{aligned} \quad (8)$$

where the boundary Γ of the domain is divided into two distinct subsets Γ_p , Γ_q such that $\Gamma_p \cup \Gamma_q = \Gamma$ and $\Gamma_p \cap \Gamma_q = 0$.

3 Cohesive fracture model

Let the complete domain be composed of a set of different homogeneous sub-domains. Within a generic one of these, a fracture can initiate or propagate under the assumption of mode I crack opening, provided that the tangential relative displacements of the fracture lips are negligible. In the process zone cohesive forces are transmitted, which are orthogonal to the fissure sides. Following the Barenblatt-Dugdale model [5, 6] and Hilleborg *et al.* proposals [7], the cohesive law is (Figure 1)

$$\sigma = \sigma_0 \left(1 - \frac{\delta_\sigma}{\delta_{\sigma cr}} \right) \quad (9)$$

σ_0 being the maximum cohesive traction (closed crack), δ_σ the relative displacement normal to the crack, $\delta_{\sigma cr}$ the maximum opening with exchange of cohesive tractions and $G = \sigma_0 \delta_{\sigma cr} / 2$ the fracture energy. Figure 1 also presents the unloading/reloading paths represented by

$$\sigma = \sigma_0 \left(1 - \frac{\delta_{\sigma 1}}{\delta_{\sigma cr}} \right) \frac{\delta_\sigma}{\delta_{\sigma 1}} \quad (10)$$

where $\delta_{\sigma 1}$ is the maximum attained opening in the previous loading process.

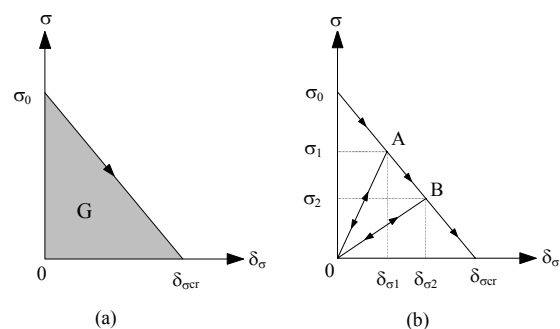


Fig. 1 Fracture energy (a) and loading/unloading law (b) for each homogeneous component

The individual homogeneous components differ only due to different values attributed to the fundamental parameters defining the mechanical behaviour as described through Eq. (9) and (10). The aspect of the constitutive relationship remains the same.

When tangential relative displacements of the sides of a fracture in the process zone cannot be disregarded, mixed mode crack opening takes place. This is usually the case with a crack moving along an interface separating two solid components. Whereas the crack path in a homogeneous medium is governed by the principal stress direction, the interface has an orientation that is generally different from the principal stress direction. The mixed cohesive mechanical model involves the simultaneous activation of normal and tangential displacement discontinuity with respect to the crack and corresponding tractions. The interaction between the two cohesive mechanisms is treated as in Margolin [8] and Dienes [9], by defining an equivalent or effective opening displacement δ and the scalar effective traction t as

$$\delta = \sqrt{\beta^{-2} \delta_\tau^2 + \delta_\sigma^2}, \quad t = \sqrt{\beta^2 t_\tau^2 + t_\sigma^2} \quad (11)$$

The resulting cohesive law is

$$\mathbf{t} = \frac{t}{\delta} (\beta^2 \delta_\tau + \delta_\sigma) \quad (12)$$

β is a suitable material parameter and the cohesive law takes the same aspect as in Figure 1, by replacing displacement and traction parameters with the corresponding effective ones. For the choice of the value of parameter β the original proposals of [8], [9] are referred to, together with reference [10].

4 SPACE-REFINEMENT STRATEGY

In the frame of h -refinement method in space and in spite of its cost, a total or partial remeshing technique is adopted in the following. For all variables, linear approximation of the field is used. To reduce computation time, the successive refinement/derefinement operations can be limited to suitable sub-domains containing the singularities zones. The dimensions of these areas and local density of discretization can be decided on the basis of the solution at the previous steps. The main reason for adopting this type of remeshing is to preserve a good mesh, which is necessary especially for modelling the transport mechanisms, even though some problems may arise for transferring data from a mesh to another. The link between the refinement and the mesh generator is the spacing function, which is point-wise updated according to the *a posteriori* calculated error. The spacing function and the ensuing node distribution is then regularized by interpolation when the new nodes are inserted. In this way the resulting mesh always present a smooth distribution of element dimensions [11].

The general scheme of the refinement procedure is presented in Fig. 2. It is important to remark that the first step is performed by the mesh generator using the multi-constrained algorithm [11], when a geometrical singularity is detected. Then the Zhu-Zienkiewicz technique is adopted [12], which relies on an *a posteriori* recovery-based error estimator. The error energy norm is calculated locally over a patch constituted by the elements, usually six, surrounding each node of the actual mesh. This error is related to the maximum permissible error. A weighting parameter is hence obtained by which the spacing function in the central node of each patch is multiplied. Note that in the used mesh generator the spacing function is defined point-wise, whereas in standard adaptive procedures the generic element is directly handled. The used approach has the advantage of producing regular and graded meshes. All field variables are involved in the adaptive procedure, however, in our applications, the stricter requirements come from the solid field.

Particular care has to be used in handling the discretization of the cohesive zone and the crack tip movement in order to avoid mesh dependency of the solution. Zhou and Molinari [13] suggest three basic rules: i) small mesh size, ii) mesh size as uniform as

possible, iii) random orientation of elements in order to avoid preferred directions. The adopted strategy guarantees all these requirements. In fact, in correspondence of the tip of the fracture we locate a point element source with strength controlled by the user or by the discretization error; uniformity of the mesh in the area surrounding the crack is assured by the interpolation of the spacing function and by the remeshing; finally, the random distribution of elements is a characteristic of Delaunay tessellation, without using highly distorted elements.

Even though the above presented mesh adaptivity algorithm is always active, for relative energy norm percentage errors typical of engineering we have found that the most pressing requirements are those of a proper representation of cohesive tractions. The same requirements allows for a good representation of the fluid field in the process zone and the fluid lag.

The refinement procedure of the process zone is as follows: the length of the process zone is *a priori* estimated for the assigned material properties and a geometry similar to the case at hand (in the application Barenblatt's theory [14] has been used). Once this length is obtained, the analyst can choose the number of elements to discretize it (element threshold number). This allows to construct a goal-oriented refinement (Fig. 3) and to control the trial advancing step Δs .

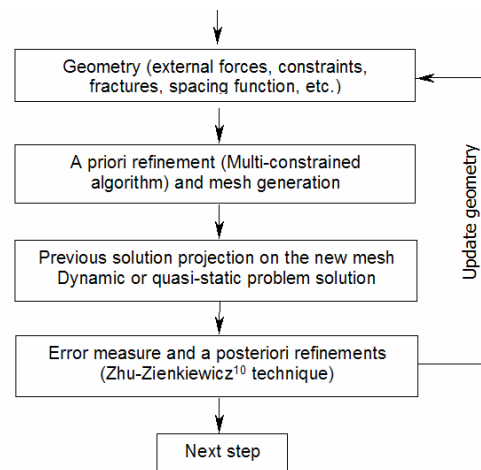


Fig. 2 General refinement procedure

As far as adaptivity in time is concerned, the importance of refinement will be assessed by repeating the complete transient analysis using reduced time steps. This is due to a lack of a suitable error estimator for non-linear coupled problems. However, this rough choice allows the assessment of the effects of space/time discretizations.

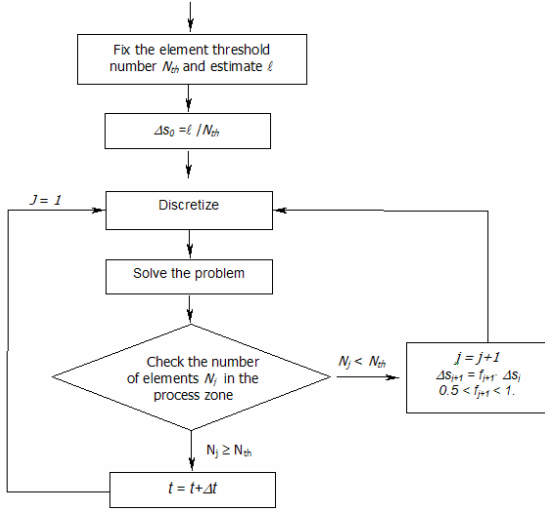


Fig. 3 Goal-oriented refinement procedure for the process zone

4 Time-refinement algorithm

The discrete form of the governing equation may be deduced from the weak formulation of the governing equations. Standard finite elements in space are combined with time discontinuous Galerkin approximation for the time-integration problem [15]. Denoting with $I_n = (t_n^-, t_{n+1}^+)$ a typical incremental time step of size $\Delta t = t_{n+1} - t_n$, the weighted residual forms are:

$$\int_{I_n} \delta \mathbf{v}^T (\mathbf{M} \dot{\mathbf{v}} + \mathbf{K} \mathbf{u} + \mathbf{L} \mathbf{p} - \mathbf{f}_u) dt + \int_{I_n} \delta \mathbf{u}^T \mathbf{K} (\dot{\mathbf{u}} - \mathbf{v}) dt + \delta \mathbf{u}^T \Big|_n \mathbf{K} (\mathbf{u}_n^+ - \mathbf{u}_n^-) dt + \delta \mathbf{v}^T \Big|_{t_n} \mathbf{M} (\mathbf{v}_n^+ - \mathbf{v}_n^-) = \mathbf{0} \quad (13)$$

$$\int_{I_n} \delta \mathbf{p}^T (\mathbf{L}^T \mathbf{v} + \mathbf{Q} \mathbf{s} + \mathbf{H} \mathbf{p} - \mathbf{f}_p) dt + \int_{I_n} \delta \mathbf{p}^T \mathbf{Q} (\dot{\mathbf{p}} - \mathbf{s}) dt + \delta \mathbf{p}^T \Big|_{t_n} \mathbf{Q} (\mathbf{p}_n^+ - \mathbf{p}_n^-) dt = \mathbf{0} \quad (14)$$

with the constraint conditions:

$$\begin{aligned} \dot{\mathbf{u}} - \mathbf{v} &= \mathbf{0} \\ \dot{\mathbf{p}} - \mathbf{s} &= \mathbf{0} \end{aligned} \quad (15)$$

Field variables at time $t \in [t_n, t_{n+1}]$ are interpolated by linear time shape functions:

$$\begin{aligned} \mathbf{u} &= N_1(t) \mathbf{u}_n + N_2(t) \mathbf{u}_{n+1} \\ \mathbf{p} &= N_1(t) \mathbf{p}_n + N_2(t) \mathbf{p}_{n+1} \\ \mathbf{v} &= N_1(t) \mathbf{v}_n + N_2(t) \mathbf{v}_{n+1} \\ \dot{\mathbf{v}} &= \dot{N}_1(t) \mathbf{v}_n + \dot{N}_2(t) \mathbf{v}_{n+1} \\ \mathbf{s} &= N_1(t) \mathbf{s}_n + N_2(t) \mathbf{s}_{n+1} \end{aligned} \quad (16)$$

Substituting equations (16) in equations (13) and (14) the following discretized equations are obtained:

$$\begin{aligned} \mathbf{u}_n &= \mathbf{u}_n^- + \frac{\Delta t}{2} (\mathbf{v}_n - \mathbf{v}_{n+1}) \\ \mathbf{u}_{n+1} &= \mathbf{u}_n^- + \frac{\Delta t}{2} (\mathbf{v}_n + \mathbf{v}_{n+1}) \end{aligned} \quad (17)$$

$$\mathbf{s}_n = \frac{1}{\Delta t} (\mathbf{p}_{n+1} + 3\mathbf{p}_n - 4\mathbf{p}_n^-)$$

$$\mathbf{s}_{n+1} = \frac{1}{\Delta t} (\mathbf{p}_{n+1} - 3\mathbf{p}_n + 2\mathbf{p}_n^-)$$

$$\begin{aligned} \left(\frac{1}{2} \mathbf{M} - \frac{5}{36} \Delta t^2 \mathbf{K} \right) \mathbf{v}_n + \left(\frac{1}{2} \mathbf{M} + \frac{1}{36} \Delta t^2 \mathbf{K} \right) + \frac{\Delta t}{3} \mathbf{L} \mathbf{p}_n + \\ + \frac{\Delta t}{6} \mathbf{L} \mathbf{p}_{n+1} = -\frac{\Delta t}{2} \mathbf{K} \mathbf{u}_n^- + \mathbf{M} \mathbf{v}_n^- + \int_{I_n} N_1(t) \mathbf{f}_u dt \\ \left(-\frac{1}{2} \mathbf{M} - \frac{7}{36} \Delta t^2 \mathbf{K} \right) \mathbf{v}_n + \left(\frac{1}{2} \mathbf{M} + \frac{5}{36} \Delta t^2 \mathbf{K} \right) + \\ \frac{\Delta t}{6} \mathbf{L} \mathbf{p}_n + \frac{\Delta t}{3} \mathbf{L} \mathbf{p}_{n+1} = -\frac{\Delta t}{2} \mathbf{K} \mathbf{u}_n^- + \int_{I_n} N_2(t) \mathbf{f}_u dt \quad (18) \\ \frac{\Delta t}{3} \mathbf{L}^T \mathbf{v}_n + \frac{\Delta t}{6} \mathbf{L}^T \mathbf{v}_{n+1} + \left(\frac{1}{2} \mathbf{Q} + \frac{\Delta t}{3} \mathbf{H} \right) \mathbf{p}_n + \\ \left(\frac{1}{2} \mathbf{Q} + \frac{\Delta t}{6} \mathbf{H} \right) \mathbf{p}_{n+1} = \mathbf{Q} \mathbf{p}_n^- + \int_{I_n} N_1(t) \mathbf{q} dt \\ \frac{\Delta t}{6} \mathbf{L}^T \mathbf{v}_n + \frac{\Delta t}{3} \mathbf{L}^T \mathbf{v}_{n+1} + \left(-\frac{1}{2} \mathbf{Q} + \Delta t \mathbf{H} \right) \mathbf{p}_n \\ + \left(\frac{1}{2} \mathbf{Q} + \frac{\Delta t}{3} \mathbf{H} \right) \mathbf{p}_{n+1} = \int_{I_n} N_2(t) \mathbf{q} dt \end{aligned}$$

The nodal displacement, velocity, pressure and flux \mathbf{u}_n^- , \mathbf{v}_n^- , \mathbf{p}_n^- and \mathbf{s}_n^- for the current step represent the unknowns at the end of the previous time step, hence in the time marching scheme are known and coincide with the initial condition for the first time step. The system of algebraic equations is solved with a monolithic approach using an optimized non-symmetric-sparse-matrix algorithm.

The error of the time-integration procedure can be defined through the jumps $[\mathbf{u}_n]$, $[\mathbf{v}_n]$, $[\mathbf{p}_n]$ and $[\mathbf{s}_n]$ of the unknowns. By adopting the total energy norms as error measure, we obtain:

$$\begin{aligned} \|\mathbf{e}_u\|_n &= \left([\mathbf{v}_n]^T \mathbf{M} [\mathbf{v}_n] + [\mathbf{u}_n]^T \mathbf{K} [\mathbf{u}_n] \right)^{\frac{1}{2}}, \\ \|\mathbf{e}_{u,p}\|_n &= \left([\mathbf{u}_n]^T \mathbf{L} [\mathbf{p}_n] \right)^{\frac{1}{2}}, \\ \|\mathbf{e}_p\|_n &= \left([\mathbf{p}_n]^T \mathbf{L}^T [\mathbf{u}_n] + [\mathbf{p}_n]^T \mathbf{H}^T [\mathbf{u}_n] \Delta t + \right. \\ &\quad \left. + [\mathbf{p}_n]^T \mathbf{Q}^T [\mathbf{u}_n] \right)^{\frac{1}{2}} \\ \|\mathbf{e}\|_n &= \max \left\{ \|\mathbf{e}_u\|_n, \|\mathbf{e}_{u,p}\|_n, \|\mathbf{e}_p\|_n \right\} \end{aligned} \quad (19)$$

The relative error is defined as [15]:

$$\eta_n = \frac{\|\mathbf{e}\|_n}{\|\mathbf{e}\|_{\max}} \quad (20)$$

where $\|\mathbf{e}\|_{\max}$ is the maximum total energy norm:

$$\|\mathbf{e}\|_{\max} = \max(\|\mathbf{e}\|_i), \quad 0 < i < n \quad (21)$$

When $\eta > \eta_{tol}$ the time step Δt_n is modified and a new $\Delta t'_n < \Delta t_n$ according to the following rule:

$$\Delta t'_n = \left(\frac{\theta \eta_{tol}}{\eta} \right)^{1/3} \Delta t_n \quad (22)$$

where $\theta < 1.0$ is a safety factor. In the following example we assume $\theta = 0.95$ and $\eta_{tol} = 0.05$. If the error is less than $\eta_{tol, min}$ the step is increased using a rule similar to Eq. (22).

5 Numerical results

The mechanical behaviour of a homogeneous soil specimen compressed by a constant vertical load has been analysed (Terzaghi's column). The specimen is shaped as a prismatic cylinder 650 mm height with a cross section 200x200 mm. The finite element mesh uses standard isoparametric 8-nodes elements; material data has been summarized in Table 1 and is represented in fig. 4.

Tab. 1

Young Modulus	60 MPa
Poisson	0.4
ρ	1800 kg/m ³
n	0.4
ρ_f	1000 kg/m ³
K_s	1e10 MPa
K_f	1e10 MPa
k_x	5.76 mm/s
k_y	5.76 mm/s
k_z	5.76 mm/s

In figure 4 the time history of the pressure in the first 50 s of the transient solution is compared between a traditional Galerkin finite element scheme and the present discontinuous Galerkin method.

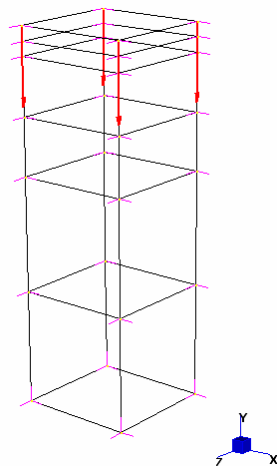


Fig. 4 Geometry of the sample

Firstly we compare the solutions obtained by means of the traditional finite difference method and the

one resulting from the application of discontinuous Galerkin approximation in time, obviously when using the same time-discretization. In the first case the nearly incompressible fluid causes a numerical oscillation of the solution; whereas with the discontinuous algorithm the spurious modes are filtered and the solution is much more accurate. In fig. 5 the time history of the liquid pressure calculated near the top of the mesh is shown. Numerical instabilities due to the nearly-incompressible-fluid condition appear with a traditional finite-differences solution; the discontinuous adaptive procedure gives much more stable and accurate results. The figure 6 shows the vertical displacement and the pressure discontinuities (at the top) before updating the time step with the time-discontinuous-adaptive-criterion. The total energy and the energy error at the base of the adaptive algorithm is displayed in fig. 7.

6 Conclusions

The proposed method is particularly flexible and very effective when a continuous change of geometrical mesh and time stepping is requested. Among the advantages of the proposed method when compared to traditional integration methods based on finite differences (with the same order of approximation) the most remarkable are the improved accuracy, the mitigation of the spurious oscillations of the solution typical in traditional time integration algorithms with incompressible fluids, the reduction of oscillations due to high modes. However, the most interesting aspect is the possibility to define an error measure based on the discontinuity of the solution at the beginning of time steps in order to activate a time stepping procedure. The drawbacks of the proposed procedure are essentially computational, in fact the number of unknowns is doubled and the final system of discretized equation turns to be non symmetric. Both these aspects can be certainly overtaken with the continuously increasing of the computational capabilities.

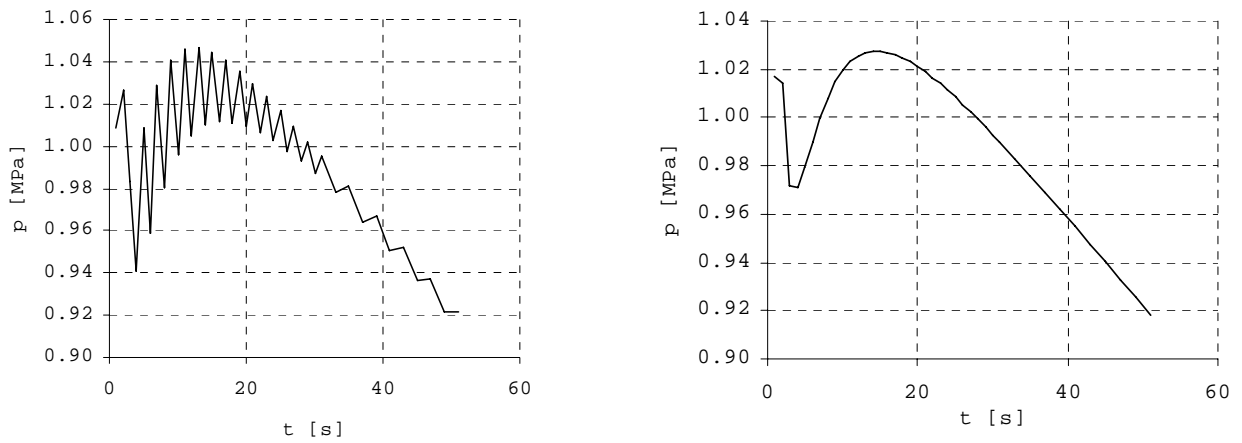


Fig. 5 Time history of pressure: finite differences solution (left) and discontinuous Galerkin fem in time (right)

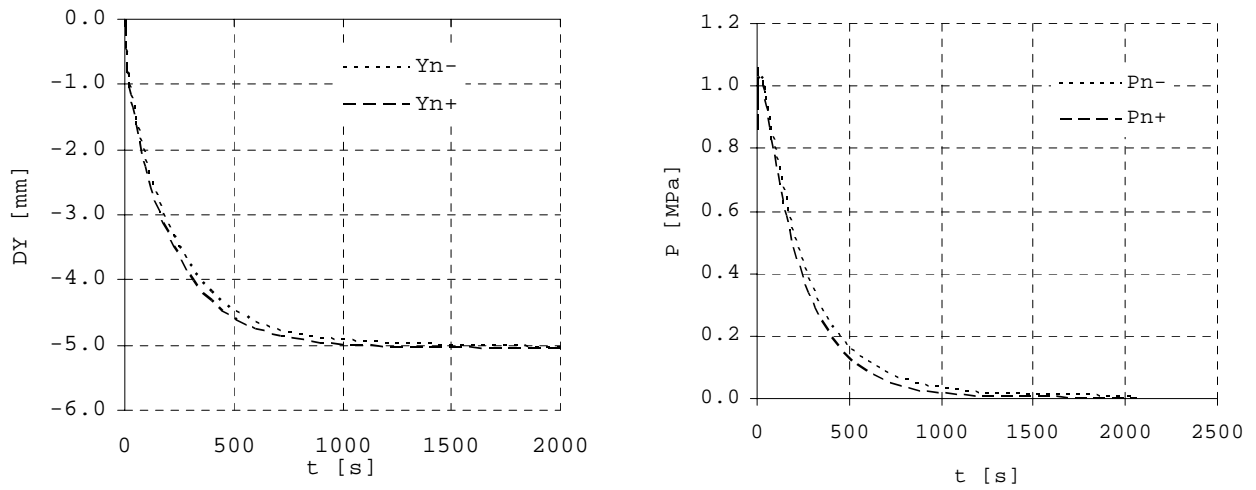


Fig. 6 Time history of vertical top displacement (left) and top pressure (right) at time t_n^- and t_n^+

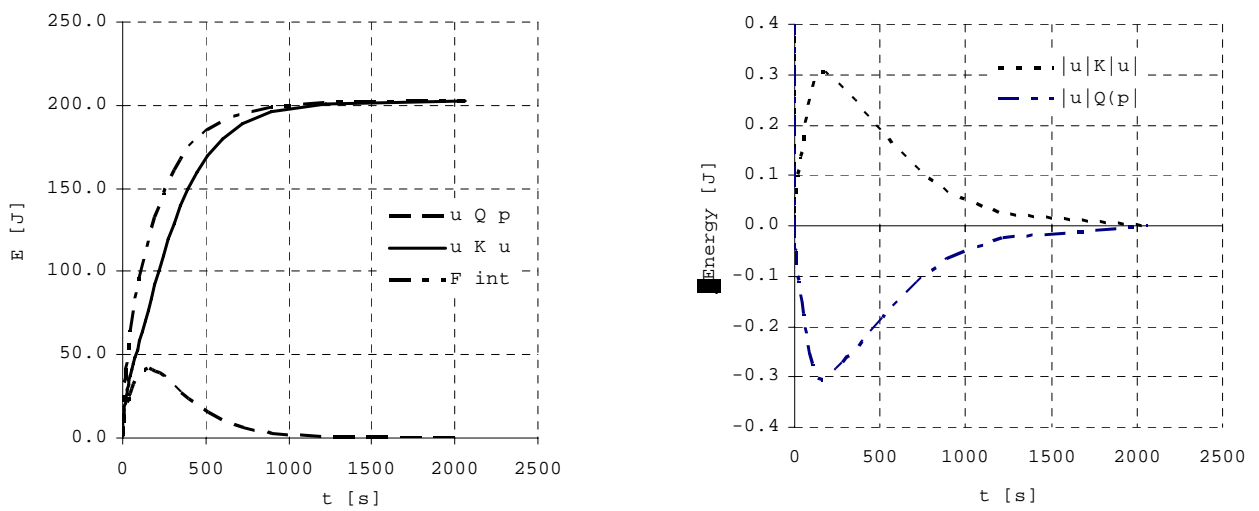


Fig. 7 Energy norms (internal energy, coupling term energy and total energy) and the energy error (right).

7 References

- [1] Zhu J.Z. and Zienkiewicz O.C., "Adaptive techniques in the finite element method", *Communications Applied Numerical Methods*, 4, 197-204, 1988.
- [2] Secchi S., Simoni L. and Schrefler B.A., "Cohesive Fracture Growth in a Thermoelastic Bi-material Medium", *Computers and Structures*, 82, 1875-1887, 2004.
- [3] Secchi S. and Simoni L., "An Improved Procedure for 2-D Unstructured Delaunay Mesh Generation", *Advances in Engineering Software*, 34, 217-234, 2003.
- [4] Lewis R.W. and Schrefler B.A., *The finite element method in the static and dynamic deformation and consolidation of porous media*, Wiley, 1998.
- [5] Barenblatt, G.I., The formation of equilibrium cracks during brittle fracture: General ideas and hypotheses. Axially-symmetric cracks. *J. Appl. Math. Mech.*, 23, 1959, 622-636.
- [6] Dugdale, D.S., Yielding of steel sheets containing slits, *J. Mech. Phys. Solids*, 8, 1960, 100-104.
- [7] Hilleborg A., Modeer M., Petersson P.E., Analysis of crack formation and crack growth in concrete by means of fracture mechanics and finite elements, *Cement and Concrete Research*, 6, 773-782, 1976.
- [8] Margolin, L.G., A generalized Griffith criterion for crack propagation, *Engineering Fracture Mechanics*, 19, 539-543, 1984.
- [9] Dienes, J.K., Comments on „A generalized Griffith criteria for crack propagation”, *Engineering Fracture Mechanics*, 23, 615-617, 1986.
- [10] Camacho G.T., Ortiz M., Computational modeling of impact damage in brittle materials, *Int. Journal of Solids and Structures*, 33, 2899-2938, 1996.
- [11] Secchi S. and Simoni L., "An Improved Procedure for 2-D Unstructured Delaunay Mesh Generation", *Advances in Engineering Software*, 34, 217-234, 2003.
- [12] Zienkiewicz O.C., Taylor R.L., *The finite element method*, Butterworth-Heinemann, 2000.
- [13] Zhou F. and Molinari J. F., "Dynamic crack propagation with cohesive elements: a methodology to address mesh dependency", *Int. J. Numerical Methods in Engineering*, 59, 1-24, 2004.
- [14] Barenblatt, G.I., "The formation of equilibrium cracks during brittle fracture: General ideas and hypotheses. Axially-symmetric cracks.", *J. Applied Mathematical Mechanics*, 23, 622-636, 1959.
- [15] Li X.D., Wiberg N.E., Structural dynamic analysis by a time-discontinuous Galerkin finite element method, *International Journal for Numerical Methods in Engineering*, 39, 2131-2152, 1996.